Supporting information for

Particle and DBPs removal efficiency and toxicity evaluation of polypropylene cotton filters in household drinking water purification system

Linlin Pan [a,b], Yuan Zhuang[b*], Ruya Chen [b,d], Yitian He [b,c], Baoyou Shi [b,c*]

a. School of Municipal and Environmental Engineering, Shandong Jianzhu University, Jinan, 250101, P R China

b. Key Laboratory of Drinking Water Science and Technology, Research Center for Eco-Environmental Sciences, Chinese Academy of Sciences, Beijing 100085, China

c. University of Chinese Academy of Sciences, Beijing 100049, China

d. School of Environmental Science and Engineering, Zhejiang Gongshang University, Hangzhou, 310012, Zhejiang, China

*Corresponding author,

Yuan Zhuang, E-mail: yuanzhuang@rcees.ac.cn,

Baoyou Shi, E-mail: byshi@rcees.ac.cn

1. Material and Methods

1.1 Water quality analysis

The excitation-emission matrix (EEM) was used to describe the DOM, which was recorded using an F-7000 fluorescence spectrophotometer (Hitachi, Chiyoda, Tokyo, Japan). Excitation wavelengths varied from 200 to 400 nm in 5 nm increments, whereas emission wavelengths were 220 to 550 nm. To eliminate the majority of the Raman scatter peaks, an EEM of Milli-Q water was prepared and subtracted from the EEM of each sample. The Raman water peak was monitored to ensure the fluorescence spectrophotometer's stability, and the fluorescence intensity was calibrated using this peak with an excitation wavelength of 350 nm (Zhang et al., 2021). The varied compositions of DOM were investigated using EEM's parallel factor (PARAFAC) methodology.

Aladdin Co. provided the PFOA (Shanghai, China). Wellington Laboratories provided a mass-labeled internal standard (Ontario, Canada). To evaluate the residual PFOA in the solution, a 50 mL water sample was taken at various time intervals and filtered using a glass fiber filter membrane (GF/F, Whatman). Oasis WAX SPE cartridges (6 cc, 150 mg, 30 m Waters) were used for sample extraction, and each water sample was spiked with 2 ng mass-labeled standards. The supporting material contains detailed information on the extraction. The quantities of PFOA were determined using an Agilent 1290 Infinity HPLC System in conjunction with an Agilent 6460 Triple

Quadrupole LC/MS System (Agilent Technologies) in negative electrospray ionization (ESI-) mode.

1.2 Toxicity evaluation

A simple, nonradioactive, colorimetric 3-(4,5-dimethylthiazol-2-yl)-2,5-diphenyltetrazolium bromide (MTT) test was performed to quantify the cell cytotoxicity of the iron particles as well as the proliferation or viability of the cells with the loose deposits(Zhuang et al., 2019). The absorbance value at 570 nm was chosen to indicate the number of live cells since dimethyl sulfoxide (DMSO) may disintegrate cell membranes. UV irradiation for 30 minutes sterilized the items used to collect and logarithmically count the LO_2 cells. After adjusting the cell suspension concentration, 100 μl of suspension was put into each well of a well plate at a rate of 2×10^4 cells per well. No iron particles were used in the control experiment. The Chinese Academy of Sciences' Shanghai Cell Bank provided the healthy human liver cells utilized in the toxicity test. The cells were cultivated in an incubator with a 5% CO_2 environment at 37°C. After 72 h, the cultural media was withdrawn. Each well received 200 μl of a 0.5 mg/ml MTT solution. The medium was withdrawn after incubation, and the formazan crystals were solubilized in the incubator for 10 minutes with 150 μl of isopropanol. A microplate reader (EPOCH2T, Biotek) was used to measure the absorbance of each well at 570 nm. The relative cell viability was obtained by averaging the results of three replicate tests. After being treated with Calcein-AM, materials were imaged using an optical microscope (DMI8, Leica) after 72 h.

1.3 DNA extraction and quantitative polymerase chain reaction (qPCR)

Divide the five-centimeter PP cotton into three layers from the inside and outside, then cut it into 2mm thick blocks that are one centimeter by one centimeter, place it in a sterile centrifuge tube, vibrate with ultrasound for 60 minutes, then make three water samples. All of the tools used in the above procedures were sterilized before being performed on the sterile operation table. According to a prior study(Jing et al., 2021; Liu et al., 2017), each sample was filtered through a sterile 0.22 m polycarbonate filter (Millipore Isopore^{TM}, USA) to collect intracellular DNA. The purified amplicons were delivered to a company (Majorbio BioTech China) for Illumina MiSeq sequencing, with the raw reads saved in the NCBI Sequence Read Archive (SRA) database (Accession Number: PRJNA669169, PRJNA669192, PRJNA669206, and PRJNA669591). The V4-V5 sections of the bacterial 16S rRNA gene were amplified using the primers 338F (5′-barcode- ACTCCTACGGGAGGCAGCAG -3′) and 806R (5′- GGACTACHVGGGTWTCTAAT -3′) (Huo et al., 2021; Liu et al., 2017; Zhang et al., 2019). The detailed PCR amplification procedures are described elsewhere(Huo et al., 2021; Jing et al., 2021; Li et al., 2020). The data are shown in Table S1 and S2.

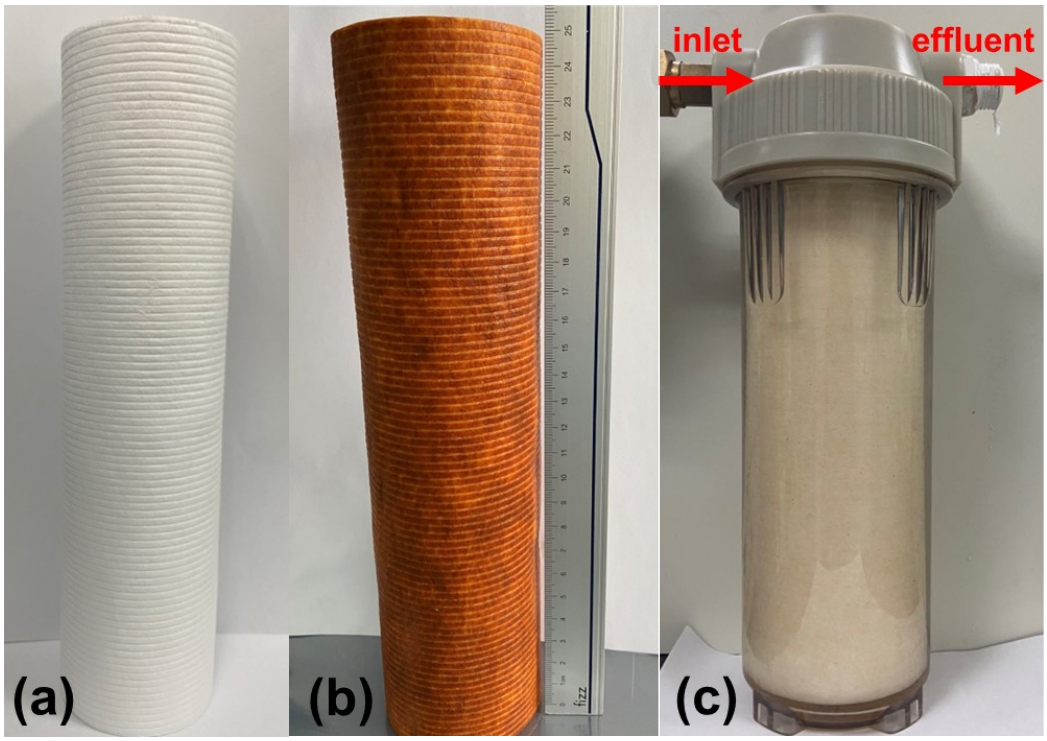

Fig. S1 New and used PCF. (a: New PCF, b: used PCF, c: PCF in use)

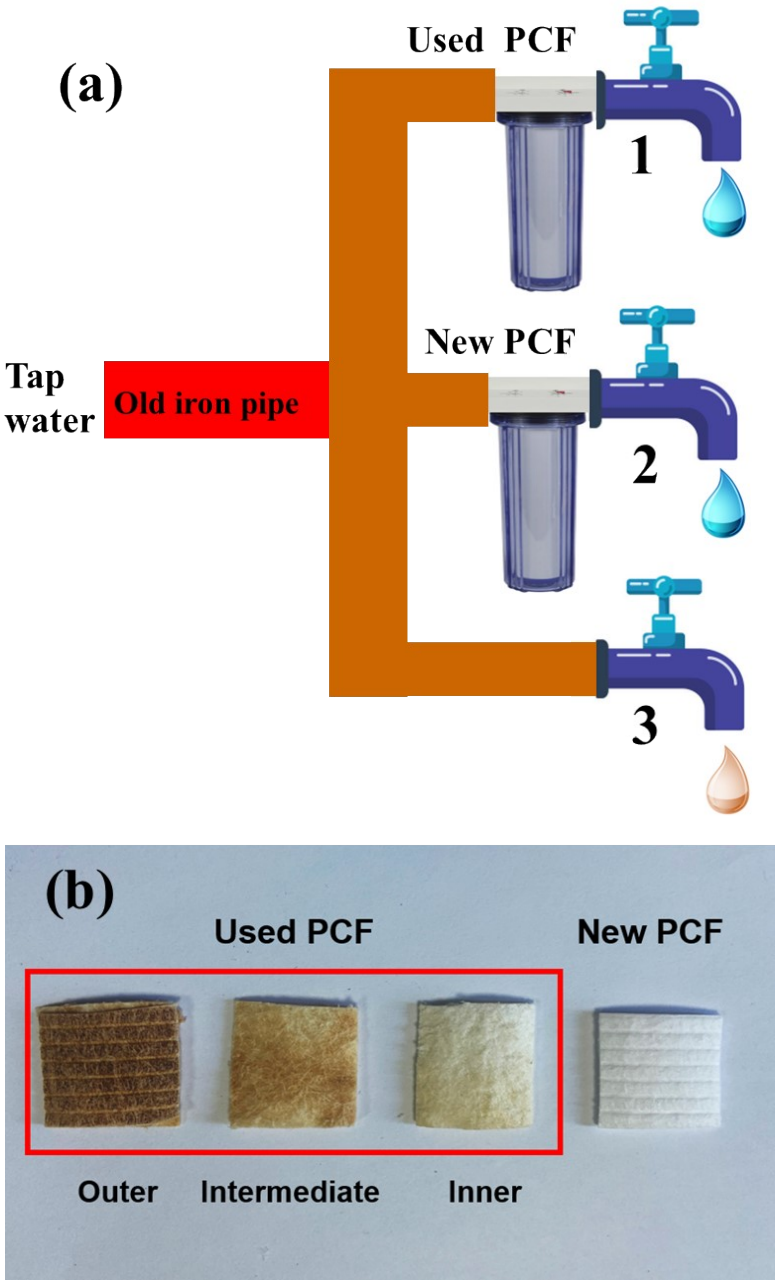

Fig.S2 (a): Schematic diagram of experimental device (b): From left to right are the outer layer of used PCF, intermediate layer of used PCF, inner layer of used PCF, and new PCF respectively.

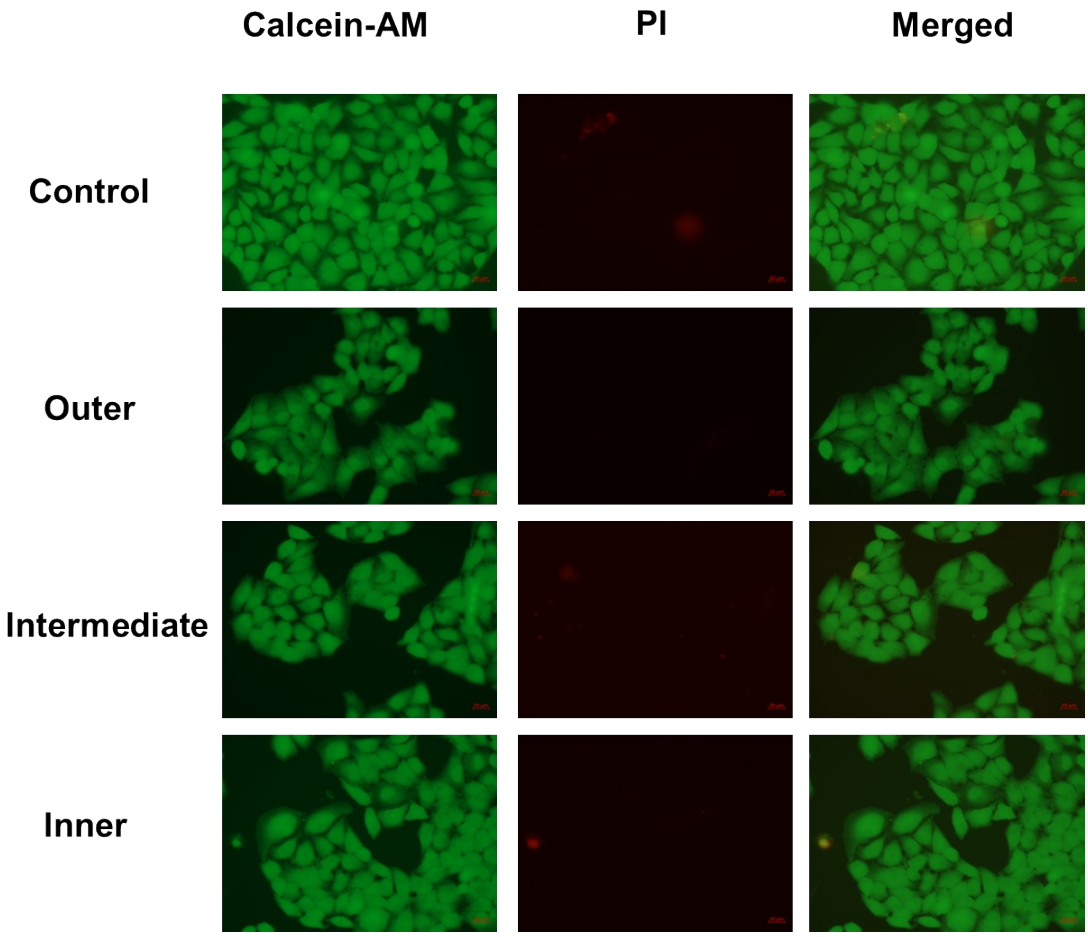

Fig.S3 Fluorescence microscopy images of cells (green: live cells; red: dead cells)

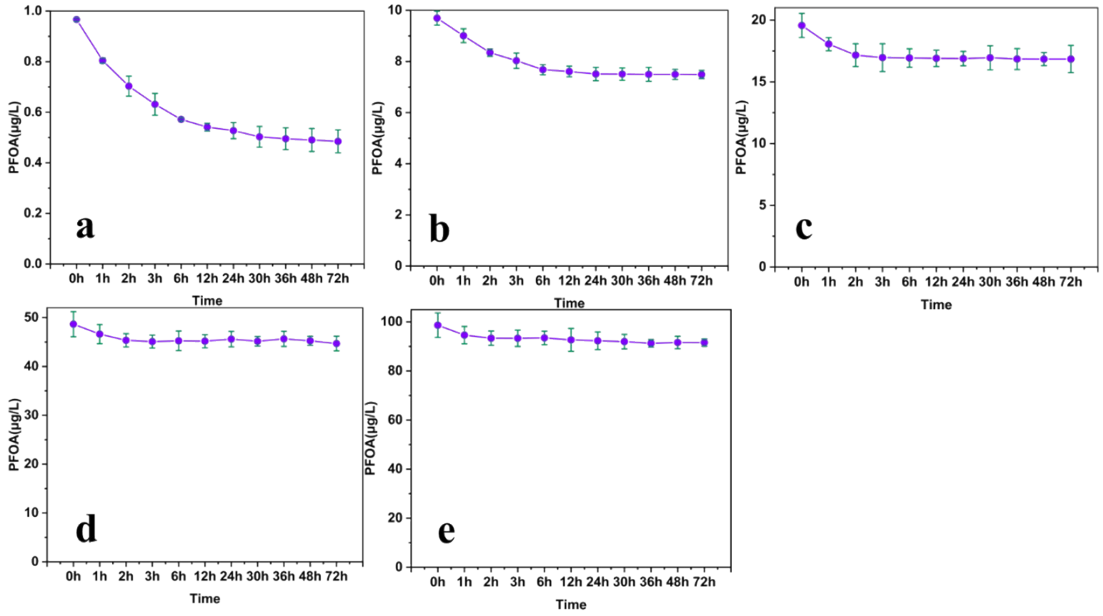

Fig.S4 The accumulation effect of 0.1g particles of the particles from outer layer of PCF added to PFOA of different concentration systems. (a: 1 μg/L, b: 10 μg/L, c: 20 μg/L, d: 50 μg/L, e: 100 μg/L)

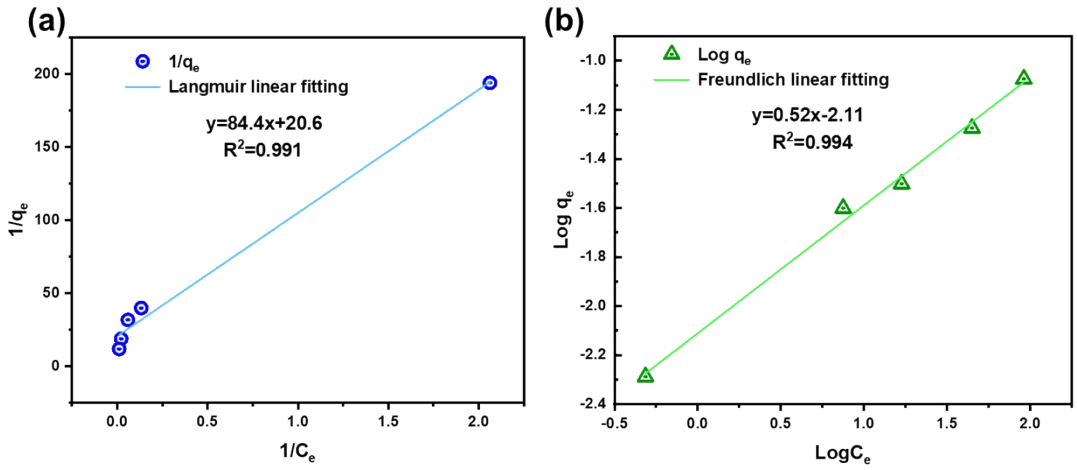

Fig. S5 Adsorption isotherms of PFOA onto particles using the Langmuir and Freundlich model (a: Langmuir model, b: Freundlich model)

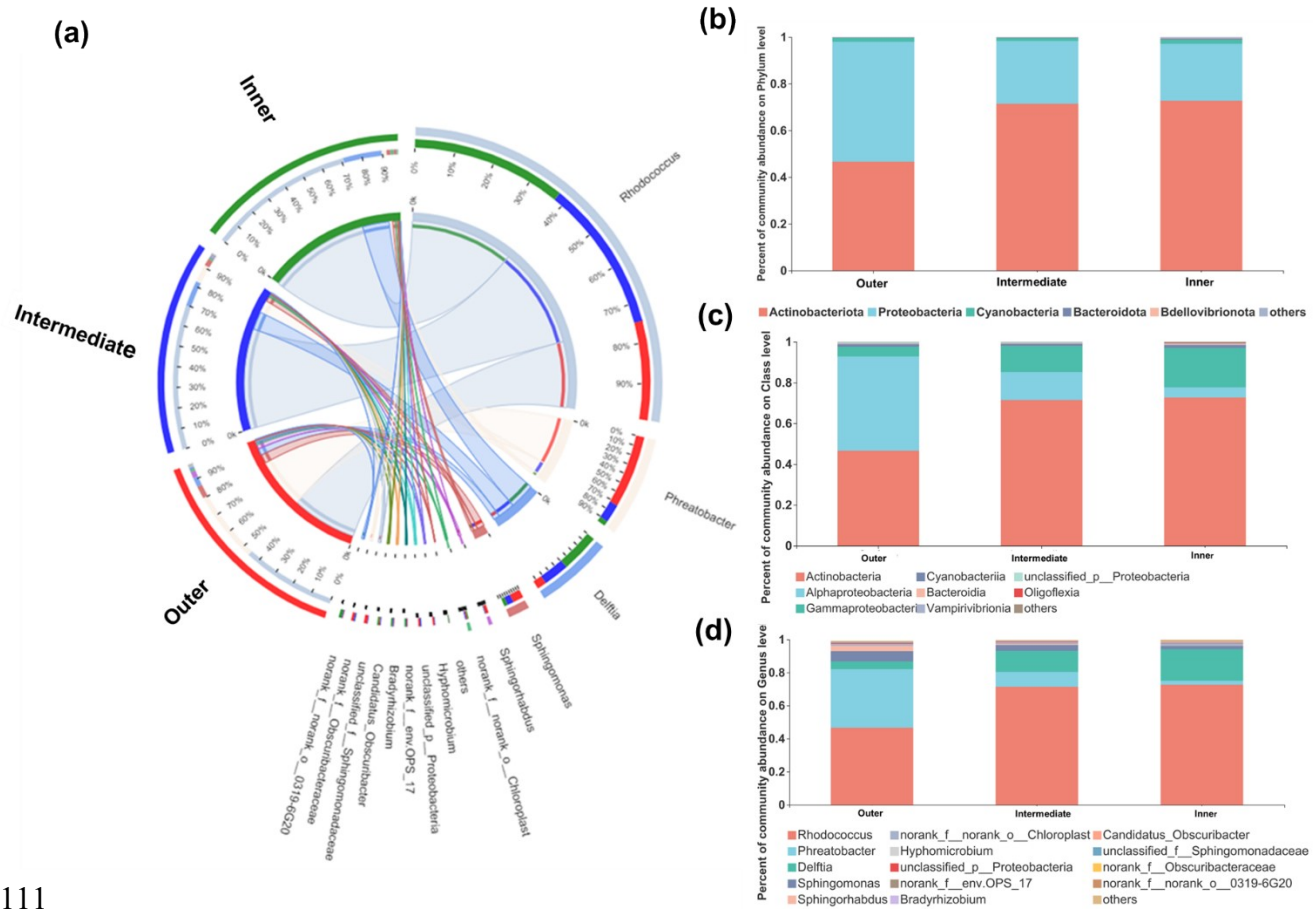

Fig.S6 Relationship between samples and species (a: the relationship between samples and species, Phylum (a) class (c) and genus (d) level community composition of three layers of PCF)

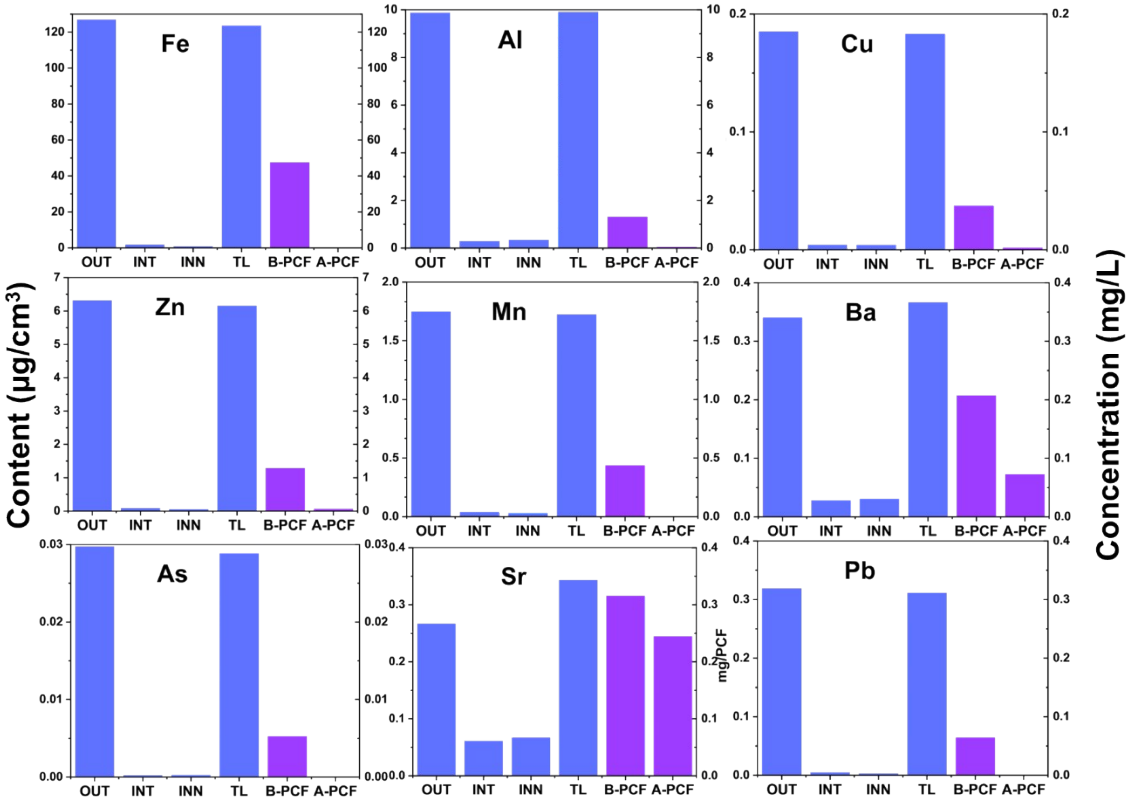

Fig. S7 Metals on each layer of PCF, concentration change of metals before and after filtration with PCF (Each figure is from left to right: OUT: outer layer, INT: intermediate layer, INN: inner layer, B-PCF: before filtration of PCF, A-PCF: after filtration of PCF)

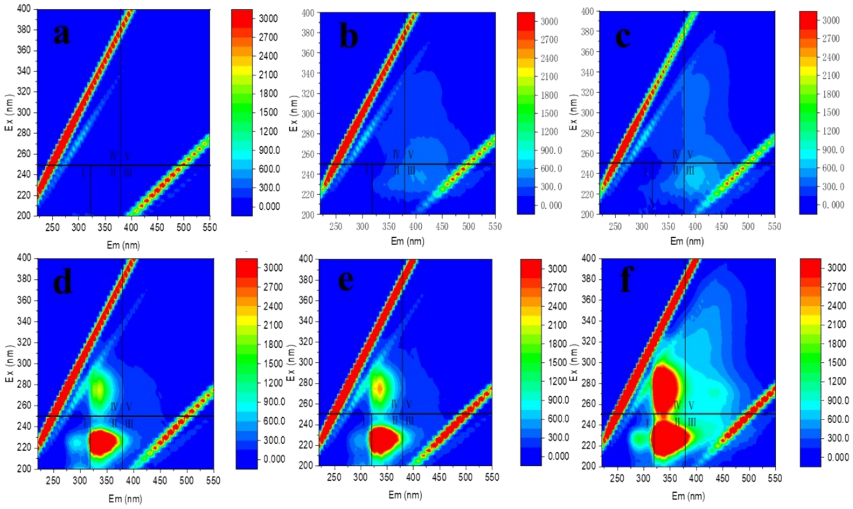

Fig. S8 EEMs on each layer of PCF, concentration change of EEMs before and after filtration with PCF (a: pure water, b: after PCF, c: before PCF, d: inner layer, e: intermediate layer, f: outer layer)

Table S1 The DNA concentration of all samples (ng/μL).

Sample	Concentration(ng/μL)
Outer layer	3.7
Intermediate layer	1.5
Inner layer	4.05±0.25
After filtration of PCF	2.80±0.20
Before filtration of PCF	1.95±0.15

149

150 T**able S2** Relative abundance of bacterial composition in biofilm samples at genus
151 level.

OTU ID	**Inner**	**Intermediate**	**Outer**
Rhodococcus	0.726511	0.714295	0.465984
Phreatobacter	0.024046	0.089672	0.354461
Delftia	0.190315	0.127461	0.046911
Sphingomonas	0.01996	0.035292	0.06244
Sphingorhabdus	0.000703	0.006548	0.031881
Chloroplast	0.014481	0.010894	0.013089
Hyphomicrobium	0.000816	0.002651	0.007638
Proteobacteria	0.000542	0.003172	0.004227
norank_f__env.OPS_17	0.003946	0.002096	0.001737
Bradyrhizobium	0.003418	0.00199	0.001343
Candidatus_Obscuribacter	0.00282	0.001364	0.001716
ProteSphingomonadaceae	2.81E-05	0.000591	0.003299
norank_f__Obscuribacteraceae	0.000239	0.00083	0.001737
norank_f__norank_o__0319-6G20	0.001653	0.000387	0.000331
norank_f__Gemmataceae	0.000443	0.000239	0.000443
unclassified_o__Rhizobiales	1.41E-05	0.000309	0.000577
unclassified_k__norank_d__Bacteria	7.74E-05	0.000352	0.000246
Nitrospira	0.000542	2.81E-05	4.22E-05
Methylotenera	0.000471	7.03E-06	5.63E-05
norank_f__Saprospiraceae	0.00038	7.03E-06	2.11E-05
DSSF69	3.52E-05	0.00012	0.000225
Haliangium	0.000316	1.41E-05	1.41E-05
Aquabacterium	0.00012	0.000148	7.03E-05
Acinetobacter	0.000239	7.03E-05	1.41E-05
norank_f__Gemmatimonadaceae	0.000295	7.03E-06	2.11E-05
Cutibacterium	0.000197	5.63E-05	7.03E-06
Terrimonas	0.000211	1.41E-05	1.41E-05
Dechloromonas	0.000197	7.03E-06	1.41E-05
Ralstonia	6.33E-05	8.44E-05	6.33E-05
JGI_0001001-H03	0.000183	0	2.81E-05
Corynebacterium	0.000113	2.81E-05	7.03E-05
norank_f__SM2D12	0.000113	2.81E-05	6.33E-05
Nevskia	5.63E-05	3.52E-05	9.85E-05
Candidatus_Alysiosphaera	0.00019	0	0
Staphylococcus	0.000105	6.33E-05	1.41E-05
Denitratisoma	0.000169	7.03E-06	0
unclassified_f__Hyphomonadaceae	2.81E-05	3.52E-05	9.14E-05
norank_f__SC-I-84	0.000148	0	0
norank_f__norank_o__norank_c__OLB14	0.00012	7.03E-06	2.11E-05
Ottowia	0.000113	2.11E-05	1.41E-05
Methylobacterium-Methylorubrum	8.44E-05	5.63E-05	7.03E-06
g__norank_f__norank_o__PLTA13	0.000105	7.03E-06	2.81E-05
norank_f__norank_o__Microtrichales	0.000113	0	2.11E-05
IMCC26207	0.000113	0	1.41E-05
Undibacterium	6.33E-05	2.81E-05	3.52E-05
norank_f__AKYH767	0.000113	7.03E-06	7.03E-06
Kouleothrix	0.00012	0	0
Pelomonas	9.14E-05	1.41E-05	7.03E-06
norank_f__Caulobacteraceae	8.44E-05	2.11E-05	7.03E-06
Conexibacter	7.74E-05	1.41E-05	1.41E-05
Burkholderia-Caballeronia-	2.81E-05	5.63E-05	1.41E-05

Paraburkholderia unclassified_f__Methylophilaceae	7.03E-05	2.11E-05	7.03E-06
CL500-3	2.81E-05	4.22E-05	2.81E-05
Candidatus_Berkiella	8.44E-05	7.03E-06	7.03E-06
Mycobacterium	5.63E-05	1.41E-05	2.81E-05
Pseudomonas	2.81E-05	7.03E-06	0

152

153

Tab.S3 Water quality parameters of red water and tap water before and after treatment with new and used PCF elements

	pH	Free chlorine /mg/L	Temperature (℃)	Conductivity / S/m	Sulfate /mg/L	Turbidity /NTU	Alkalinity /mg/L	Larson Index	Total particles
Tap water	7.95	0.65	27.1	465	51.5	0.44	120.3	1.34	10137
Red water	7.87	0.55	27.5	485	52.1	5.23	83.6	1.93	3652
After used PCF	7.91	0.40	27.4	473	51.1	0.89	109.3	1.45	2968
After new PCF	7.93	0.62	27.2	450	49.6	0.29	118.6	1.30	336

$$\frac{1}{q_e} = \frac{1}{q_m K_L C_e} + \frac{1}{q_m} \quad \text{(S1)}$$

where C_e is the PFOA concentration in solution (μg/L) at equilibrium, q_e denotes the amount adsorbed at equilibrium (mg/g), q_m is the maximum adsorption capacity of particles (mg/g), and K_L is the adsorption constant at equilibrium.

$$\log q_e = \log K_f + \frac{1}{n} \log C_e \quad \text{(S2)}$$

where K_f is a constant associated with the adsorption capacity and 1/n is an empirical parameter relating the outer affinity, which varies with the heterogeneity of outer site energy distribution.

References:

Huo, L., Pan, L., Chen, R., Shi, B., Wang, H., He, S., 2021. Effects of disinfectants and particles on the occurrence of different microorganisms in drinking water distribution systems. Environmental science water research & technology 7(5), 983-992.

Jing, Z., Lu, Z., Mao, T., Cao, W., Wang, W., Ke, Y., Zhao, Z., Wang, X., Sun, W., 2021. Microbial composition and diversity of drinking water: A full scale spatial-temporal investigation of a city in northern China. Sci. Total Environ. 776, 145986.

Li, W., Tan, Q., Zhou, W., Chen, J., Li, Y., Wang, F., Zhang, J., 2020. Impact of substrate material and chlorine/chloramine on the composition and function of a young biofilm microbial community as revealed by high-throughput 16S rRNA sequencing. Chemosphere 242, 125310.

Liu, G., Tao, Y., Zhang, Y., Lut, M., Knibbe, W., van der Wielen, P., Liu, W., Medema, G., van der Meer, W., 2017. Hotspots for selected metal elements and microbes accumulation and the corresponding water quality deterioration potential in an unchlorinated drinking water distribution system. Water Res. 124, 435-445.

Liu, J., Shentu, H., Chen, H., Ye, P., Xu, B., Zhang, Y., Bastani, H., Peng, H., Chen, L., Zhang, T., 2017. Change regularity of water quality parameters in leakage flow conditions and their relationship with iron release. Water Res. 124, 353-362.

Zhang, J., Li, W., Chen, J., Wang, F., Qi, W., Li, Y., 2019. Impact of disinfectant on bacterial antibiotic resistance transfer between biofilm and tap water in a simulated distribution network. Environ. Pollut. 246, 131-140.

Zhang, Y., Lu, Z., Zhang, Z., Shi, B., Hu, C., Lyu, L., Zuo, P., Metz, J., Wang, H., 2021. Heterogeneous Fenton-like reaction followed by GAC filtration improved removal efficiency of NOM and DBPs without adjusting pH. Sep. Purif. Technol. 260, 118234.

Zhuang, Y., Han, B., Chen, R., Shi, B., 2019. Structural transformation and potential toxicity of iron-based deposits in drinking water distribution systems. Water Res. 165, 114999.